LETTERS

An essential role for a CD36-related receptor in pheromone detection in *Drosophila*

Richard Benton[1]†, Kirsten S. Vannice[1]† & Leslie B. Vosshall[1]

The CD36 family of transmembrane receptors is present across metazoans and has been implicated biochemically in lipid binding and transport[1]. Several CD36 proteins function in the immune system as scavenger receptors for bacterial pathogens and seem to act as cofactors for Toll-like receptors by facilitating recognition of bacterially derived lipids[2–4]. Here we show that a *Drosophila melanogaster* CD36 homologue, Sensory neuron membrane protein (SNMP), is expressed in a population of olfactory sensory neurons (OSNs) implicated in pheromone detection. SNMP is essential for the electrophysiological responses of OSNs expressing the receptor OR67d to (*Z*)-11-octadecenyl acetate (*cis*-vaccenyl acetate, cVA), a volatile male-specific fatty-acid-derived pheromone that regulates sexual and social aggregation behaviours[5–8]. SNMP is also required for the activation of the moth pheromone receptor HR13 by its lipid-derived pheromone ligand (*Z*)-11-hexadecenal[9], but is dispensable for the responses of the conventional odorant receptor OR22a to its short hydrocarbon fruit ester ligands. Finally, we show that SNMP is required for responses of OR67d to cVA when ectopically expressed in OSNs not normally activated by pheromones. Because mammalian CD36 binds fatty acids[10], we suggest that SNMP acts in concert with odorant receptors to capture pheromone molecules on the surface of olfactory dendrites. Our work identifies an unanticipated cofactor for odorant receptors that is likely to have a widespread role in insect pheromone detection. Moreover, these results define a unifying model for CD36 function, coupling recognition of lipid-based extracellular ligands to signalling receptors in both pheromonal communication and pathogen recognition through the innate immune system.

Insect odorant receptors represent a novel class of polytopic membrane proteins unrelated to vertebrate G-protein-coupled chemosensory receptors[11,12]. The functional insect odorant receptor is a heteromer of a ligand-binding subunit and the highly conserved OR83b co-receptor, which mediates transport to sensory cilia[11,13–15]. Little is known about how this complex recognizes odours and evokes neuronal depolarization. To isolate novel components involved in insect olfactory detection, we used a bioinformatic approach to identify molecules that exhibit the same insect-specific orthology and olfactory-specific tissue expression as these receptors (Fig. 1). Two-thousand one-hundred and thirty-five *Drosophila* genes with insect-specific orthologues were identified by comparing the fruit fly (*Drosophila melanogaster*), mosquito (*Anopheles gambiae*) and eight non-insect genomes using the OrthoMCL algorithm (Fig. 1a)[16]. Broadly expressed genes were excluded by selecting only the 616 genes with fewer than two expressed sequence tags. We recovered all classes of known insect chemosensory genes, including odorant receptors, gustatory receptors, odorant and other chemosensory binding proteins, and putative odour-degrading enzymes (Fig. 1b and Supplementary Table 1). The remaining genes were classified on the basis of predicted protein domains (Fig. 1b and

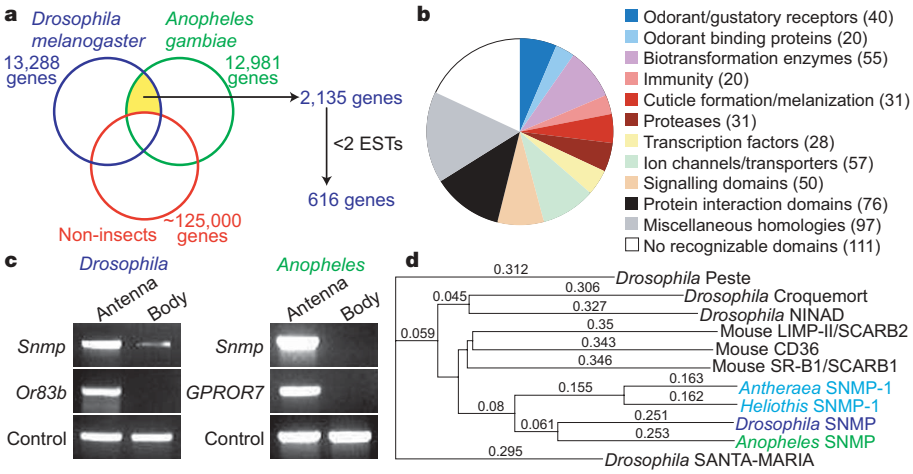

Figure 1 | A comparative genomics screen for olfactory molecules identifies *Drosophila* SNMP, a CD36-related receptor. **a**, Summary of bioinformatic screen. EST, expressed sequence tag. **b**, Pie chart of putative functions of genes retrieved from the screen. **c**, RT–PCR of *Snmp* homologues in *Drosophila* and *Anopheles*. Control RT–PCR products: *Cam* (*Drosophila*) and *rps7* (*Anopheles*). **d**, Phylogenetic tree of insect SNMPs and related *Drosophila* and mammalian CD36 proteins. Values are uncorrected ('*p*') distance.

[1]Laboratory of Neurogenetics and Behaviour, The Rockefeller University, 1230 York Avenue, Box 63, New York, New York 10065, USA. †Present addresses: Center for Integrative Genomics, Genopode Building, University of Lausanne, CH-1015 Lausanne, Switzerland (R.B.); Johns Hopkins Bloomberg School of Public Health, 615 North Wolfe Street, Baltimore, Maryland 21205, USA (K.S.V.).

Supplementary Table 1) and included many implicated in immunity and defence.

Three-hundred and thirty-nine uncharacterized genes were screened for selective expression in the antenna—the major olfactory organ of *Drosophila*—by reverse transcriptase–polymerase chain reaction (RT–PCR). Of these, we focus here on *Snmp*, an antennal-enriched gene related to the CD36 receptor family (Fig. 1c). The *Anopheles* homologue of *Snmp* was also antennal-specific (Fig. 1c), consistent with the previously described olfactory-specific expression pattern of the silk moth (*Antheraea polyphemus*) homologue *Snmp-1* (ref. 17). SNMPs form an insect-specific sub-group of the CD36 family (Fig. 1d), explaining how *Drosophila Snmp* emerged from our bioinformatic screen.

In the antenna, *Snmp* was found prominently expressed in a lateral-distal population of OSNs that co-express *Or83b* (Fig. 2b)[11,13–15], in non-neuronal support cells that surround these OSNs, and in support cells elsewhere in the antenna and chemosensory organs on the proboscis (Fig. 2b, and data not shown). Genetic labelling of SNMP-expressing OSNs with mouse CD8 fused to green fluorescent protein (CD8–GFP) revealed that these neurons target nine glomeruli in the antennal lobe (Fig. 2c)[18,19]—DA1, VA1d, VA1l/m, DL3, DA4m, DA4l, DA2, DC3 and DC1—corresponding to those innervated by OSNs of the trichoid sensilla, which are involved in pheromone detection[20,21].

Using a peptide antibody, SNMP was found concentrated in trichoid sensory cilia, where it co-localized with OR83b (Fig. 2d), but only at very low levels in the cell bodies and axons (Fig. 2d, and data not shown), similar to moth SNMP-1 (ref. 17). We did not observe SNMP in non-trichoid OSNs, but it was expressed in support cells throughout the antenna (Fig. 2d). All anti-SNMP immunoreactivity was abolished in an *snmp*-null mutant (see below), confirming antibody specificity. Although the localization of SNMP in OSN cilia was similar to that of odorant receptors, it did not depend on OR83b when we expressed a functional SNMP–GFP fusion protein in OSNs innervating basiconic sensilla (Fig. 2e, and Supplementary Fig. 1). Therefore, SNMP ciliary trafficking is independent of both specific ligand-binding odorant receptors and OR83b. We examined whether SNMP might still contact odorant receptors in trichoid cilia by using the fluorescent protein fragment complementation assay[11]. We generated and functionally verified SNMP and OR83b bearing complementary fragments of a yellow fluorescent protein (YFP) reporter (Fig. 2f and Supplementary Fig. 1). Reconstitution of the fluorescent YFP signal in sensory cilia was only observed when both fusion proteins were expressed (Fig. 2f). As the YFP fragments do not self-associate, this reconstitution could only result if SNMP and OR83b were brought into close proximity (<80 Å), providing evidence that SNMP is closely apposed to, although not necessarily directly interacting with, odorant receptors in the sensory compartment.

We generated null mutants in *Snmp* by gene targeting[22] (Fig. 3a–d). *snmp* mutants are viable and fertile with no gross morphological or locomotor defects. We examined the function of SNMP in the subpopulation of trichoid sensilla innervated by neurons expressing OR67d—the best-characterized *Drosophila* pheromone receptor that recognizes cVA[8,21,23]. In *snmp* mutants, neither the expression of *Or67d* nor the ciliary localization of GFP–OR67d or OR83b was affected (Fig. 3c, e) and axonal projections of *snmp* mutant OR67d-expressing neurons to the antennal lobe were wild type (Fig. 3f). The expression of LUSH, an odorant-binding protein secreted by trichoid sensilla support cells into the lymph[6] was normal (Fig. 3g). Thus *Snmp* is dispensable for the development of trichoid OSNs and support cells.

We investigated whether the responses of OR67d neurons to cVA stimulation were altered in *snmp* mutants. The relatively low

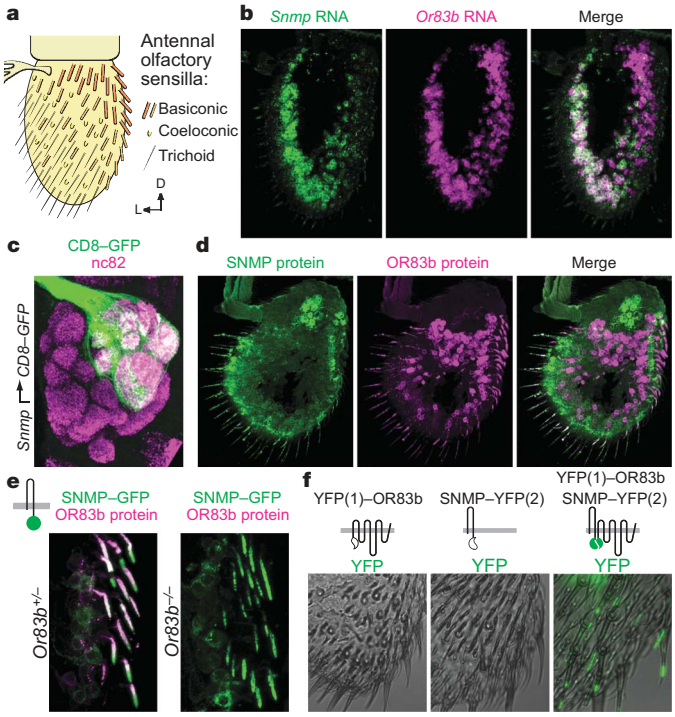

Figure 2 | SNMP localizes to sensory cilia of pheromone-sensitive OSNs. **a**, Olfactory sensilla distribution on the third antennal segment. Tissue orientation is always dorsal up, lateral left. **b**, RNA *in situ* hybridization of *Snmp* and *Or83b* on a wild-type antennal section. **c**, Immunostaining of CD8–GFP (anti-GFP) and neuropil (nc82) of a whole-mount brain of an *Snmp*-promoter-*VP22–GAL4/UAS-CD8–GFP* animal. **d**, Immunostaining of SNMP and OR83b on a wild-type antennal section. **e**, Immunostaining of SNMP–GFP (anti-GFP) and OR83b on antennal sections of control heterozygous (left) and homozygous (right) *Or83b*-null mutant animals. A model of SNMP–GFP is at the top left. **f**, Intrinsic YFP fluorescence in antennal sections of animals expressing YFP(1)–OR83b, SNMP–YFP(2) or both fusion proteins, as indicated. *Drosophila* genotypes are in Methods.

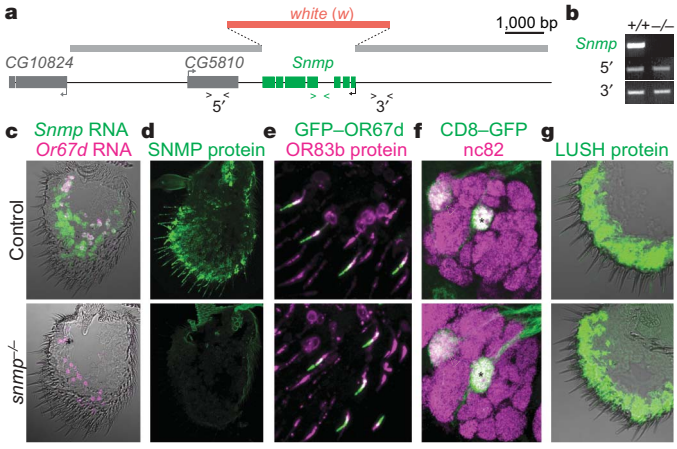

Figure 3 | Genetic analysis of *Snmp*. **a**, *Snmp* genomic locus and gene-targeting strategy. **b**, PCR confirmation of homozygous *snmp*-null mutant (*snmp*^{1}) using primer pairs indicated in **a**. **c**, RNA *in situ* hybridization of *Snmp* and *Or67d* in antennal sections of control heterozygous (*snmp*^{1}/+) or homozygous *snmp* mutant (*snmp*^{1}/*snmp*^{2}) animals. **d**, Immunostaining of SNMP on antennal sections of control wild-type or homozygous *snmp* mutant (*snmp*^{1}/*snmp*^{2}) animals. **e**, Immunostaining of GFP–OR67d (anti-GFP) and OR83b on antennal sections of control heterozygous or homozygous *snmp* mutant animals. **f**, Immunostaining of CD8–GFP-labelled OR67d-expressing axon termini (anti-GFP) and neuropil (nc82) on whole-mount brains of control heterozygous and homozygous *snmp* mutant animals. *Or67d-GAL4* labels two glomeruli[18,19]: DA1 (receives input from OR67d-expressing OSNs) and VA6 (black asterisk; receives input from OR82a-expressing OSNs), the latter originally interpreted by us as co-convergence[19] but later shown to be due to ectopic expression of *Or67d-GAL4* in OR82a neurons[8]. **g**, Immunostaining of LUSH on antennal sections of control wild-type or homozygous *snmp* mutant (*snmp*^{1}/*snmp*^{2}) animals.

spontaneous activity of the OR67d neuron was observable as a sparse distribution of action potentials of uniform amplitude (Fig. 4a). On stimulation with cVA, wild-type neurons responded with a robust train of action potentials in a dose-dependent manner (Fig. 4a, b). *snmp* mutant neurons displayed no cVA-evoked electrophysiological responses at any concentration tested (Fig. 4a, b), but showed an increase in spontaneous activity (Fig. 4a). Both spontaneous and stimulus-evoked responses were fully restored by expression of the *Snmp* rescuing transgene in OR67d-expressing neurons (Fig. 4a, b, and Supplementary Fig. 2), but not by expression in support cells surrounding these neurons (Fig. 4a, b, and Supplementary Fig. 2). Expression of a distinct *Drosophila* CD36-related protein, NINAD, in OR67d-expressing neurons did not rescue electrophysiological defects of *snmp* mutants (data not shown). Thus, SNMP has an essential, cell-autonomous and specific function in OR67d-expressing neurons in mediating responses to cVA.

cVA detection is also dependent on LUSH and the OR67d/OR83b heteromeric receptor complex[6,8,23] (data not shown), suggesting that SNMP acts with these proteins in a signalling pathway. In contrast to *snmp* mutants, however, loss of *lush*, *Or67d* or *Or83b* severely decreased spontaneous activity of these neurons (Fig. 4c, d)[6,8]. Double-mutant analysis of this spontaneous activity phenotype revealed that *Snmp* is epistatic to *lush,* because OR67d-expressing neurons retained high levels of spontaneous activity in animals lacking both SNMP and LUSH (Fig. 4c, d). In contrast, *snmp Or83b* double mutants were, like *Or83b*, electrically silent (Fig. 4c, d). Although the mechanism by which spontaneous activity is regulated in *Drosophila* OSNs is unknown, our genetic analysis indicates that SNMP may act downstream of LUSH and upstream of, or in parallel with, odorant receptors in the generation of action potentials.

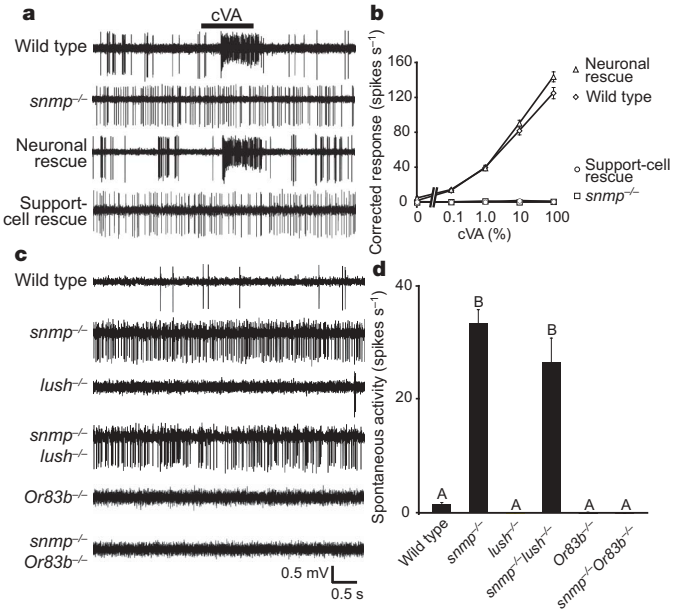

Figure 4 | SNMP mediates electrophysiological responses to cVA. **a**, Representative traces of extracellular recordings of OR67d neurons stimulated with 10% cVA in wild-type, *snmp* mutant, neuronal rescue, and support-cell rescue animals. Bar above traces marks stimulus time (1 s). Traces are from female flies, but no significant sex-specific cVA responses are observed. **b**, Dose–response curves for cVA in the genotypes in **a**. Mean responses are plotted (±s.e.m.; $n = 39$–47 sensilla; ≤4 sensilla per animal, mixed genders). *snmp* mutant and support-cell *Snmp* rescue are highly significantly different from wild-type and neuronal rescue animals at all concentrations of cVA (ANOVA; $P < 0.0001$). **c**, Representative traces of spontaneous activity in OR67d neurons in wild-type, *snmp* mutant, *lush* mutant, *snmp lush* double-mutant, *Or83b* mutant and *snmp Or83b* double mutant animals. **d**, Quantification of mean spontaneous activity in the genotypes in **c** (±s.e.m.; $n = 16$–20, male flies). Bars labelled with different letters are highly significantly different (ANOVA; $P < 0.0001$).

To investigate the specificity of SNMP function, we ectopically expressed in OR67d neurons a second receptor, OR22a, which is responsive to fruit esters, such as ethyl butyrate and pentyl acetate[24]. Although chemically related to cVA, OR22a ligands lack the long hydrophobic tail of this fatty-acid-derived pheromone (Fig. 5a). Ectopic expression of OR22a in wild-type OR67d-expressing neurons conferred responses to a panel of known OR22a ligands in addition to the endogenous cVA response (Fig. 5a, b), but not to a control odour, geranyl acetate, which activates neither OR67d nor OR22a (ref. 25). In *snmp* mutants, ectopic OR22a-dependent responses were unaffected, but all cVA responses were lost (Fig. 5a, b). The broad expression of SNMP in trichoid OSNs indicates that it might have a general function in pheromone detection. Because no other volatile pheromones have been identified in *Drosophila*, we tested whether SNMP is required for the activation of the moth (*Heliothis virescens*) pheromone receptor HR13 by (*Z*)-11-hexadecenal[9], a component of the sex pheromone blend of this species. As previously observed, expression of HR13 in OR67d-expressing neurons conferred responsiveness to this pheromone[8] (Fig. 5c, d). This response was almost completely abolished in *snmp* mutants and restored by transgenic rescue of *Snmp* (Fig. 5c, d). Together, these experiments reveal a specific and conserved function for SNMP in mediating pheromone-evoked neuronal activity. OR67d and HR13 share <15% amino acid identity and their ligands have chemically distinct head groups, suggesting that it is the fatty-acid-derived hydrocarbon tail common to these pheromones that necessitates SNMP.

Finally, we asked whether SNMP is required for the activation of OR67d by cVA in neurons not normally responsive to pheromones. We ectopically expressed OR67d in basiconic OSNs that lack the endogenous OR22a ligand-binding odorant receptor, but retain OR83b (ref. 24). All action potentials in these neurons can therefore be ascribed to OR67d/OR83b activity. *Or22a* mutant neurons expressing OR67d without SNMP exhibited spontaneous firing, but did not respond to cVA (Fig. 5e, f). In contrast, when OR67d was co-expressed with SNMP, significant responses to this pheromone were observed (Fig. 5e, f); compared to the responses of native OR67d neurons, the frequency of action potentials was lower and exhibited slower rise and decay rates (Fig. 5e, f). Such differences may be due to the absence in basiconic sensilla of LUSH or odour-degrading enzymes specialized to inactivate pheromone molecules[26].

Through a bioinformatic screen for insect olfactory transduction molecules, we have identified *Drosophila* SNMP as a CD36-related receptor broadly expressed in pheromone-sensing neurons, which is an essential co-factor for detection of the fatty-acid-derived pheromone cVA. As mammalian CD36 has an important biochemical function in binding and membrane translocation of fatty acids we suggest SNMP directly captures pheromone molecules on the surface of OSN cilia—possibly retrieving them from odorant-binding proteins in the extracellular milieu—and facilitates their transfer to the odorant-receptor–OR83b complex (Fig. 5g). A recent study showed OR67d ectopically expressed without SNMP could be activated by cVA when the pheromone was directly applied to the sensillar cuticle overlying the OSN[21], indicating that pheromone receptors can be directly stimulated by ligand. When pheromones are presented in an air stream to the receptor in its native environment, however, SNMP (and odorant-binding proteins[6]) are essential. We suggest that the combination of molecular specializations of pheromone-sensing trichoid neurons together contribute to the sensitivity of these cells and that SNMP-related proteins function in the detection of many insect pheromones.

The mechanistic basis of CD36 ligand interactions and signalling is still poorly understood in any biological system. Our results have three important general implications. First, we show that SNMP has a specific role in the detection of fatty-acid-derived odour ligands. Because other CD36-related receptors are involved in binding and transport of lipid-based molecules, for example in the

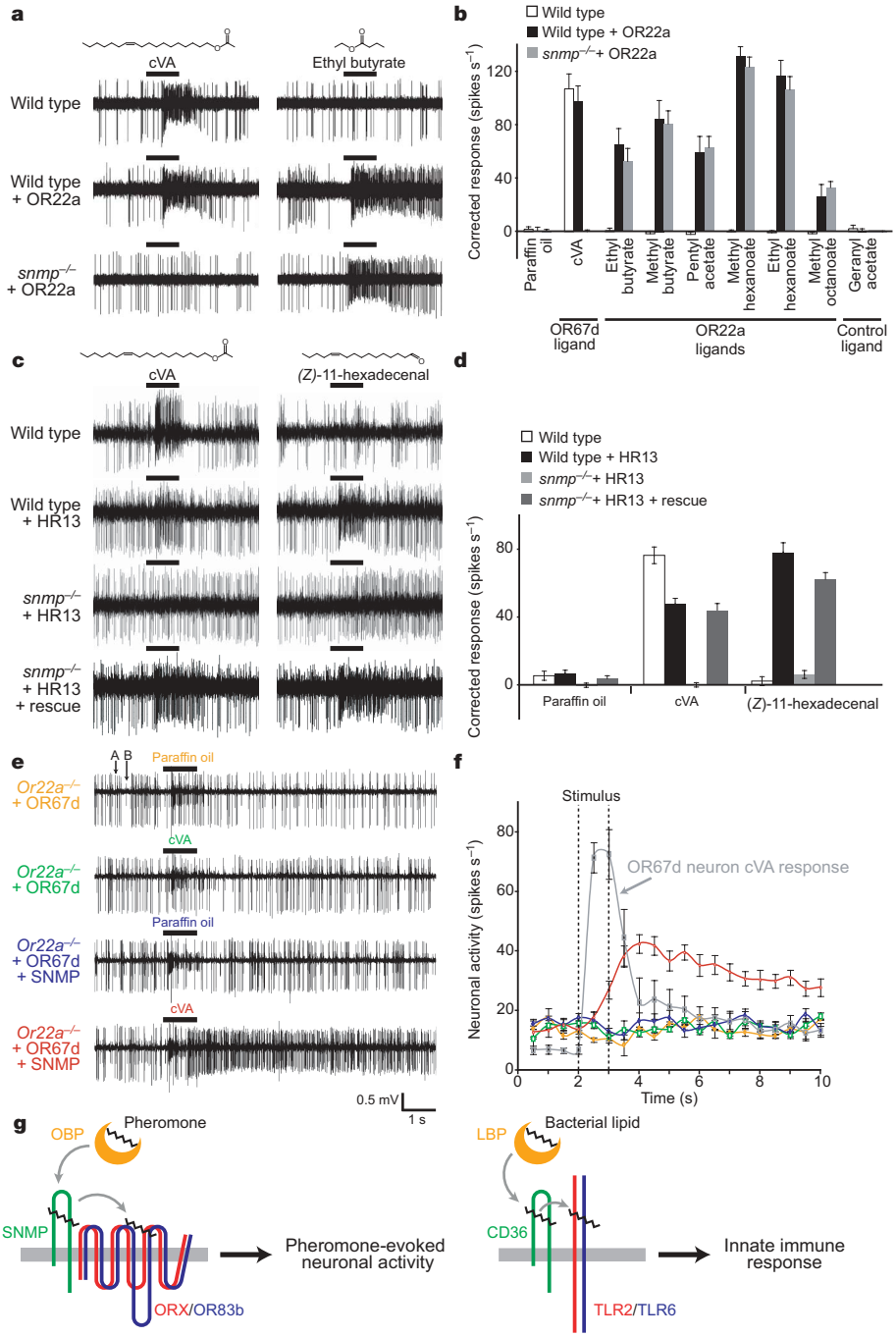

Figure 5 | SNMP is specifically required, and sufficient, for pheromone detection. **a**, Representative traces from OR67d neurons stimulated with 10% cVA or 10% ethyl butyrate in wild-type, wild-type + ectopic OR22a, or *snmp*-null mutant + ectopic OR22a animals. Bars above traces mark stimulus time (1 s). Structures of compounds are depicted at the top. **b**, Quantification of responses to cVA and OR22a ligands in the genotypes in **a**. Mean responses are plotted (±s.e.m.; $n = 16$, female flies). Responses of wild-type and *snmp*-mutant OR67d-expressing neurons ectopically expressing OR22a are highly significantly different for cVA (ANOVA; $P < 0.0001$) but not to any OR22a ligand (ANOVA; $P > 0.4149$). Geranyl acetate is a control odour that does not stimulate OR67d or OR22a. **c**, Representative traces from OR67d neurons stimulated with 10% cVA or 100% (*Z*)-11-hexadecenal in wild-type, wild-type + ectopic HR13, *snmp*-null mutant + ectopic HR13, or *snmp*-null mutant + ectopic HR13 + *Snmp* rescue animals. Bars above traces mark stimulus time (1 s). Structures of pheromones are depicted at the top. **d**, Quantification of responses to cVA and (*Z*)-11-hexadecenal in the genotypes in **c**. Mean responses are plotted (±s.e.m.; $n = 17$–19, female flies). Responses to (*Z*)-11-hexadecenal of wild-type and *snmp*-mutant OR67d neurons ectopically expressing HR13 are highly significantly different (ANOVA; $P < 0.0001$). HR13-dependent responses to (*Z*)-11-hexadecenal of *Snmp* rescue animals are highly significantly different from both wild-type and *snmp* mutant responses (ANOVA; $P < 0.0001$), indicating partial rescue. **e**, Representative traces from *Or22a* mutant neurons expressing OR67d alone or OR67d and SNMP, stimulated with control solvent paraffin oil or 100% cVA. Bars above traces mark stimulus time (1 s). OR22a neurons reside in basiconic sensilla with two neurons, visible as two distinct amplitudes (labelled A and B) of action potentials: responses of OR67d in *Or22a* mutant neurons are represented by the larger amplitude. The neuron with smaller amplitude action potentials responds to both control and cVA stimuli. **f**, Peristimulus time histograms for the genotype and stimulus combinations in **e**, using the same colour scheme. Endogenous OR67d neuron response to 100% cVA is in grey. Mean responses are plotted (±s.e.m.; $n = 9$–12, mixed genders). The activity of *Or22a* mutant neurons expressing both OR67d and SNMP and stimulated with cVA is highly significantly different between time-points 3–9 s to *Or22a* mutant neurons expressing OR67d alone and/or when stimulated with paraffin oil (ANOVA; $P < 0.0001$). **g**, Model of mechanistic parallels between insect pheromone detection and bacterial pathogen detection. Extracellular LBPs (liposaccharide-binding proteins) may be functionally analogous to odorant-binding proteins (OBPs). ORX is any of the ligand-binding *Drosophila* pheromone receptors.

mammalian intestine[1], this protein family may represent specialized receptors for extracellular fatty ligands of diverse biological origin and function. Second, we show that SNMP acts in concert with other transmembrane odorant receptors in OSN cilia in mediating pheromone-evoked activity. Because CD36 was previously shown to act as a co-receptor for Toll-like receptors[2], we suggest that CD36-related proteins have obligate transmembrane partners in all their cellular roles.

Finally, our results reveal a molecular parallel in the mechanisms of intraspecific recognition through pheromone detection and pathogen recognition through the innate immune system (Fig. 5g). CD36 proteins in both invertebrates and vertebrates have been implicated in the recognition of specific lipid-derived products from bacterial cell walls, and coupling of this recognition through Toll-like receptors to initiate the innate immune response[2–4]. Notably, mammalian CD36 has been proposed as a candidate fat taste receptor[27]. Common molecular recognition mechanisms in immune and chemosensory systems may therefore be widespread.

METHODS SUMMARY

Bioinformatics. Insect-specific orthologues were identified using the OrthoMCL server (http://orthomcl.cbil.upenn.edu/cgi-bin/OrthoMclWeb.cgi)[16]. Gene targeting of *Snmp* was performed essentially as described[13]. Two null mutants, *snmp*^{1} and *snmp*^{2}, arising from different starting insertions of the targeting construct were analysed.

Histology and immunocytochemistry. Two-colour *in situ* RNA hybridization[19] and immunofluorescence on antennal sections or whole-mount brains[11,13] were performed as described. A rabbit polyclonal antibody against SNMP was raised against the synthetic peptide TNPATNPATHHKMEHRERY and affinity-purified by Proteintech Group.

Electrophysiology and odorants. Extracellular recordings in single sensilla of 2–8-day-old flies were performed essentially as described[13]. High-purity odorants were obtained from Sigma-Aldrich, except cVA (purity ~99%) obtained from Pherobank.

Full Methods and any associated references are available in the online version of the paper at www.nature.com/nature.

Received 11 June; accepted 1 October 2007.
Published online 17 October 2007.

1. Ge, Y. & Elghetany, M. T. CD36: a multiligand molecule. *Lab. Hematol.* **11,** 31–37 (2005).
2. Hoebe, K. *et al.* CD36 is a sensor of diacylglycerides. *Nature* **433,** 523–527 (2005).
3. Philips, J. A., Rubin, E. J. & Perrimon, N. *Drosophila* RNAi screen reveals CD36 family member required for mycobacterial infection. *Science* **309,** 1251–1253 (2005).
4. Stuart, L. M. *et al.* Response to *Staphylococcus aureus* requires CD36-mediated phagocytosis triggered by the COOH-terminal cytoplasmic domain. *J. Cell Biol.* **170,** 477–485 (2005).
5. Bartelt, R. J., Schaner, A. M. & Jackson, L. L. *cis*-Vaccenyl acetate as an aggregation pheromone in *Drosophila melanogaster. J. Chem. Ecol.* **11,** 1747–1756 (1985).
6. Xu, P., Atkinson, R., Jones, D. N. & Smith, D. P. *Drosophila* OBP LUSH is required for activity of pheromone-sensitive neurons. *Neuron* **45,** 193–200 (2005).
7. Ejima, A. *et al.* Generalization of courtship learning in *Drosophila* is mediated by *cis*-vaccenyl acetate. *Curr. Biol.* **17,** 599–605 (2007).
8. Kurtovic, A., Widmer, A. & Dickson, B. J. A single class of olfactory neurons mediates behavioural responses to a *Drosophila* sex pheromone. *Nature* **446,** 542–546 (2007).
9. Grosse-Wilde, E., Gohl, T., Bouche, E., Breer, H. & Krieger, J. Candidate pheromone receptors provide the basis for the response of distinct antennal neurons to pheromonal compounds. *Eur. J. Neurosci.* **25,** 2364–2373 (2007).
10. Bonen, A. *et al.* Regulation of fatty acid transport by fatty acid translocase/CD36. *Proc. Nutr. Soc.* **63,** 245–249 (2004).
11. Benton, R., Sachse, S., Michnick, S. W. & Vosshall, L. B. Atypical membrane topology and heteromeric function of *Drosophila* odorant receptors *in vivo. PLoS Biol.* **4,** e20 (2006).
12. Wistrand, M., Kall, L. & Sonnhammer, E. L. A general model of G protein-coupled receptor sequences and its application to detect remote homologs. *Protein Sci.* **15,** 509–521 (2006).
13. Larsson, M. C. *et al. Or83b* encodes a broadly expressed odorant receptor essential for *Drosophila* olfaction. *Neuron* **43,** 703–714 (2004).
14. Nakagawa, T., Sakurai, T., Nishioka, T. & Touhara, K. Insect sex-pheromone signals mediated by specific combinations of olfactory receptors. *Science* **307,** 1638–1642 (2005).
15. Neuhaus, E. M. *et al.* Odorant receptor heterodimerization in the olfactory system of *Drosophila melanogaster. Nature Neurosci.* **8,** 15–17 (2005).
16. Li, L., Stoeckert, C. J. Jr & Roos, D. S. OrthoMCL: identification of ortholog groups for eukaryotic genomes. *Genome Res.* **13,** 2178–2189 (2003).
17. Rogers, M. E., Sun, M., Lerner, M. R. & Vogt, R. G. Snmp-1, a novel membrane protein of olfactory neurons of the silk moth *Antheraea polyphemus* with homology to the CD36 family of membrane proteins. *J. Biol. Chem.* **272,** 14792–14799 (1997).
18. Couto, A., Alenius, M. & Dickson, B. J. Molecular, anatomical, and functional organization of the *Drosophila* olfactory system. *Curr. Biol.* **15,** 1535–1547 (2005).
19. Fishilevich, E. & Vosshall, L. B. Genetic and functional subdivision of the *Drosophila* antennal lobe. *Curr. Biol.* **15,** 1548–1553 (2005).
20. Kaissling, K. E. Peripheral mechanisms of pheromone reception in moths. *Chem. Senses* **21,** 257–268 (1996).
21. van der Goes van Naters, W. & Carlson, J. R. Receptors and neurons for fly odors in *Drosophila. Curr. Biol.* **17,** 606–612 (2007).
22. Gong, W. J. & Golic, K. G. Ends-out, or replacement, gene targeting in *Drosophila. Proc. Natl Acad. Sci. USA* **100,** 2556–2561 (2003).
23. Ha, T. S. & Smith, D. P. A pheromone receptor mediates 11-*cis*-vaccenyl acetate-induced responses in *Drosophila. J. Neurosci.* **26,** 8727–8733 (2006).
24. Dobritsa, A. A., van der Goes van Naters, W., Warr, C. G., Steinbrecht, R. A. & Carlson, J. R. Integrating the molecular and cellular basis of odor coding in the *Drosophila* antenna. *Neuron* **37,** 827–841 (2003).
25. Hallem, E. A. & Carlson, J. R. Coding of odors by a receptor repertoire. *Cell* **125,** 143–160 (2006).
26. Ishida, Y. & Leal, W. S. Rapid inactivation of a moth pheromone. *Proc. Natl Acad. Sci. USA* **102,** 14075–14079 (2005).
27. Laugerette, F. *et al.* CD36 involvement in orosensory detection of dietary lipids, spontaneous fat preference, and digestive secretions. *J. Clin. Invest.* **115,** 3177–3184 (2005).

Supplementary Information is linked to the online version of the paper at www.nature.com/nature.

Acknowledgements We thank R. Fenster and S. Katz for expert technical assistance; W. Jones for training in electrophysiology; M. Ditzen for providing spike analysis software; P. Morozov of the Columbia Genome Centre and AMDeC Bioinformatics Core Facility for programing to permit batch retrieval of insect-specific orthologues and expressed sequence tags; E. Zdobnov for providing a *D. melanogaster/A. gambiae* orthologue data set; P. Howell and M. Q. Benedict of the CDC and MR4 for mosquitoes; D. Smith for reagents; B. Dickson for sharing unpublished fly reagents; S. Piccinotti for graphic design; R. Vogt for discussions; and M. Heiman, K. Lee, S. Martin, K. Scott and members of the Vosshall laboratory for comments on the manuscript. R.B. was supported by an EMBO Long-Term Fellowship and the Helen Hay Whitney Foundation. This work was supported by grants to L.B.V. from the NIH and the McKnight Endowment Fund for Neuroscience.

Author Contributions R.B. and K.S.V. performed the screen for olfactory genes. R.B. carried out all other experiments and analysed the data. R.B. and L.B.V. together designed the experiments, interpreted the results, produced the figures and wrote the paper.

Author Information Reprints and permissions information is available at www.nature.com/reprints. Correspondence and requests for materials should be addressed to L.B.V. (leslie@mail.rockefeller.edu).

METHODS

Bioinformatics. Insect-specific orthologues were identified using the OrthoMCL DB server (http://orthomcl.cbil.upenn.edu/cgi-bin/OrthoMclWeb.cgi)[16], by comparing the predicted complete proteomes (in April 2004) of *Drosophila melanogaster*, *Anopheles gambiae*, *Homo sapiens*, *Mus musculus*, *Caenorhabditis elegans*, *Saccharomyces cerevisiae*, *Arabidopsis thaliana*, *Escherichia coli*, *Plasmodium falciparum* and *Plasmodium yoelii*. A supplementary data set of insect-specific orthologues was obtained from the *Anopheles gambiae* genome-sequencing project[28]. Expressed sequence tag numbers for the corresponding *Drosophila* genes were downloaded from Flybase (http://flybase.bio.indiana.edu/) in June 2004. Protein sequences were manually curated using BLAST (http://www.ncbi.nlm.nih.gov/BLAST/) and SMART (http://smart.embl-heidelberg.de) servers. *Snmp* was previously curated by Flybase/NCBI as CG7000-RA under accession number NM_142696. The best-fit phylogenetic tree in Fig. 1d was generated using the neighbour-joining algorithm in MacVector v9.0 with default parameters.

Molecular biology. Complementary DNA was synthesized from insect tissues using the Absolutely RNA Microprep Kit (Stratagene) and Superscript First-Strand Synthesis System (Invitrogen). Gene-specific primers for RT–PCR were designed using Primer3 (ref. 29) to amplify ~500 bp spanning at least one intron. All plasmid constructs were generated by amplification of the desired cDNA or genomic fragments with primers containing flanking restriction sites using the Expand High Fidelity PLUS PCR system (Roche) and Oregon-R antennal or appendage cDNA or genomic DNA as templates. PCR products were T:A cloned into pGEM-T Easy (Promega), sequenced and subcloned into appropriate vectors as detailed below: *Snmp*-promoter-*VP22–GAL4*: the *Snmp* 5.412 kb promoter region (nucleotides 16,998,115–16,992,704 in GenBank accession AE014297) was subcloned into *pVP22-GAL4* (ref. 30). *lush*-promoter-*GAL4*: the *lush* 0.959 kb promoter region (nucleotides 19,599,310–19,598,352 in GenBank accession AE014296) was subcloned into pCaSpeR-AUG-*GAL4* (ref. 30). *UAS-Snmp*: full-length *Snmp* open reading frame (GenBank accession NM_142696) was subcloned into pUAST (ref. 31). *UAS-Snmp–GFP*: full-length *Snmp* open reading frame without termination codon was subcloned 5′ of *EGFP* (Clontech) in pUAST. *UAS-Snmp–YFP(2)*: full-length *Snmp* open reading frame without termination codon was subcloned upstream of DNA encoding a 10 amino acid linker $[(GGGGS)_2]$ and a carboxy-terminal YFP fragment of YFP(2) in pUAST (ref. 11). *UAS-Or67d*: full-length open reading frame of *Or67d* was subcloned in pUAST. *UAS-GFP–Or67d*: full-length open reading frame of *Or67d* was subcloned 3′ of *EGFP* (without termination codon) in pUAST. *Snmp* targeting construct: 5′ and 3′ homologous arms (16,998,850–16,993,851 and 16,991,435–16,986,436 of GenBank accession AE014297, respectively) were subcloned to flank the *white* reporter gene in CMC105 (ref. 13). The gene structure in Fig. 3a was generated using Genepalette v1.2 (ref. 32).

Insect strains. *Drosophila* stocks were maintained on conventional cornmeal-agar-molasses medium under a 12 h light:12 h dark cycle at 25 °C. Wild-type Berlin (M. Heisenberg) was used for electrophysiological experiments and the wild-type Oregon-R strain was used for histology. Mutant alleles and transgenic lines used: $Or83b^1$, $Or83b^2$ (ref. 13), $lush^1$ (ref. 33), $Or22a/b^{\Delta halo}$ (ref. 24), *Or67d-GAL4* (ref. 19), *Or83b-GAL4* (ref. 34), *Or22a-GAL4* (ref. 19), *UAS-YFP(1)–Or83b* (ref. 11), *UAS-CD8–GFP* (ref. 35), *UAS-Or22a* (ref. 13), *UAS-HR13* (ref. 8), *UAS-ninaD* (ref. 36), *70FLP,70I-SceI/Cyo* and *70FLP* (ref. 37).

Specific genotypes of flies in the figures are listed below. Figure 2e: *Or83b-GAL4/UAS-Snmp–GFP*;$Or83b^1$/+ (left) *Or83b-GAL4/UAS-Snmp–GFP*;$Or83b^1/Or83b^2$ (right). Figure 2f: *Or67d-GAL4,UAS-YFP(1)–Or83b/+* (left), *Or67d-GAL4/UAS-Snmp–YFP(2)*;$snmp^1/snmp^2$ (centre), *Or67d-GAL4,UAS-YFP(1)–Or83b/UAS-Snmp–YFP(2)*;$snmp^1$,$Or83b^2/snmp^2$,$Or83b^1$ (right). Figure 3e: *Or67d-GAL4/UAS-GFP–Or67d*;$snmp^1$/+ (top) *Or67d-GAL4/UAS-GFP–Or67d*;$snmp^1/snmp^2$ (bottom). Figure 3f: *Or67d-GAL4/UAS-CD8–GFP*;$snmp^1$/+ (top) *Or67d-GAL4/UAS-CD8–GFP*;$snmp^1/snmp^2$ (bottom). Figure 4a: *Or67d-GAL4/+*; $snmp^1/snmp^2$ (second trace) *Or67d-GAL4/UAS-Snmp*;$snmp^1/snmp^2$ (third trace) *lush-GAL4/UAS-Snmp*;$snmp^1/snmp^2$ (bottom trace). Figure 4c: $snmp^1/snmp^2$ (second trace) $lush^1/lush^1$ (third trace) $lush^1$,$snmp^1/lush^1$,$snmp^2$ (fourth trace) $Or83b^1/Or83b^2$ (fifth trace) $snmp^1$,$Or83b^2/snmp^2$,$Or83b^1$ (bottom trace). Figure 5a: *Or67d-GAL4/UAS-Or22a* (middle) *Or67d-GAL4/UAS-Or22a*;$snmp^1/snmp^2$ (bottom). Figure 5c: *Or67d-GAL4/UAS-HR13* (second trace) *Or67d-GAL4/UAS-HR13*; $snmp^1/snmp^2$ (third trace) *Or67d-GAL4,UAS-Snmp/UAS-HR13*;$snmp^1/snmp^2$ (bottom trace). Figure 5e: $Or22a/b^{\Delta halo}/Or22a/b^{\Delta halo}$;*Or22a-GAL4,UAS-Or67d/+* (top two traces) $Or22a/b^{\Delta halo}/Or22a/b^{\Delta halo}$;*Or22a-GAL4,UAS-Or67d/UAS-Snmp* (bottom two traces).

Adult mosquitoes (*Anopheles gambiae* G3 strain; MRA-112) were obtained from MR4 (www.mr4.org) through the Centers for Disease Control and Prevention.

Gene targeting screen. Gene targeting of *Snmp* was performed essentially as described[13,38], using five independent insertions of the targeting construct. From approximately 200,000 F_2 progeny, at least 6 null mutants were obtained, which were confirmed by PCR on genomic DNA preparations from homozygous mutant animals amplifying fragments corresponding to 16,990,010–16,990,525 (5′) 16,992,709–16,993,129 (*Snmp*) and 16,994,279–16,994,757 (3′) in GenBank accession AE014297. Two of these, $snmp^1$ and $snmp^2$, arising from different starting insertions of the targeting construct, were retained for phenotypic analysis.

Histology and immunocytochemistry. Two-colour *in situ* RNA hybridization was performed essentially as described[19] using *Or83b*-FITC, *Or67d*-DIG, and *Snmp*-DIG or -FITC RNA probes. Immunofluorescence on antennal sections or whole-mount brains was performed as described[11,13]. Primary antibodies: rabbit anti-OR83b EC2, 1:5,000 (ref. 13), rabbit anti-LUSH, 1:1,000 (ref. 33), mouse monoclonal nc82, 1:10 (R. Stocker), rabbit anti-GFP, 1:1,000 (Molecular Probes), mouse anti-GFP 1:500 (Molecular Probes). A rabbit polyclonal antibody against SNMP was raised against the synthetic peptide TNPATNPATHHKMEHRERY (corresponding to the C-terminal 19 amino acids), affinity-purified by Proteintech Group and used at 1:1,000. Secondary antibodies: Alexa488- and Cy3-conjugated anti-mouse IgG or anti-rabbit IgG 1:100 or 1:1,000 for whole-mount brains and antennal sections, respectively (Molecular Probes; Jackson Immunoresearch). All microscopy was performed using a Zeiss LSM 510 Laser Scanning Confocal Microscope. For the Protein Fragment Complementation assay, the intrinsic fluorescence signal of reconstituted YFP was detected in fixed samples by excitation with an Argon Laser (excitation wavelength 488 nm) and collection of the emitted light with Band Pass filter 505–530.

Electrophysiology and odorants. Extracellular recordings in single sensilla of 2–8-day-old flies were performed essentially as described[13,38,39]. Ten microlitres of odorant was added to a 6 mm filter paper disk (Whatman), which was placed inside a 1 ml tuberculin syringe (Becton, Dickinson and Company). A charcoal-filtered airflow (35 ml s^{-1}) was used to deliver odours to the preparation through a 10 ml serological pipette that was trimmed to remove the tapered tip, and the cut end positioned 15 mm away from the preparation. Half this airflow was diverted through the odour syringe during odour stimulation periods (1 s) under the control of the Syntech CS-55 Stimulus controller. cVA (purity ~99%) was obtained from Pherobank. Other odorants were obtained from Sigma-Aldrich at high purity. Chemical Abstracts Service (CAS) numbers: ethyl butyrate (105-54-4), methyl butyrate (623-42-7), pentyl acetate (628-63-7), methyl hexanoate (106-70-7), ethyl hexanoate (123-66-0), methyl octanoate (111-11-5), geranyl acetate (105-87-3), (*Z*)-11-hexadecenal (53939-28-9). Odorants were diluted to 10% in paraffin oil, except cVA, which was used at a range of dilutions (as indicated in the figures), methyl hexanoate and ethyl hexanoate, which were used at 1%, and (*Z*)-11-hexadecenal, which was used at 100%. Trichoid sensilla innervated by OR67d neurons are proximally distributed on the antenna and can be unambiguously identified by extracellular electrophysiological recordings of individual sensilla because they are unique in housing only a single OSN. We found that the onset of cVA responses varied slightly (usually <200 ms) between animals of the same genotype recorded on different days, most probably owing to small variations in the position of the odour delivery apparatus relative to the preparation. For quantification of responses, we therefore determined the time of onset of the response of a control wild-type sensillum to 100% cVA for each recording session. Corrected responses for all recordings in the same session were quantified by counting spikes in a 0.5 s window from this time point, subtracting the number of spontaneous spikes in a 0.5 s window before stimulation, and doubling the result to obtain spikes s^{-1}. Spontaneous activity was quantified by counting the spikes in a 5 s window without stimulus, and dividing by 5 to obtain spikes s^{-1}. Peristimulus time histograms (PSTHs) were generated by counting the numbers of spikes in 0.5 s bins from 2 s before 7 s after odour stimulation for each trial, using custom software written by M. Ditzen in IDL. These values were then averaged across all trials. After verifying that responses were normally distributed, we compared all genotypes for a given experiment by ANOVA, with genotype as the main effect, and adjusted the alpha level for planned post-hoc means comparisons.

28. Zdobnov, E. M. *et al.* Comparative genome and proteome analysis of *Anopheles gambiae* and *Drosophila melanogaster*. *Science* **298**, 149–159 (2002).
29. Rozen, S. & Skaletsky, H. Primer3 on the WWW for general users and for biologist programmers. *Methods Mol. Biol.* **132**, 365–386 (2000).
30. Vosshall, L. B., Wong, A. M. & Axel, R. An olfactory sensory map in the fly brain. *Cell* **102**, 147–159 (2000).
31. Brand, A. H. & Perrimon, N. Targeted gene expression as a means of altering cell fates and generating dominant phenotypes. *Development* **118**, 401–415 (1993).
32. Rebeiz, M. & Posakony, J. W. GenePalette: a universal software tool for genome sequence visualization and analysis. *Dev. Biol.* **271**, 431–438 (2004).
33. Kim, M. S., Repp, A. & Smith, D. P. LUSH odorant-binding protein mediates chemosensory responses to alcohols in *Drosophila melanogaster*. *Genetics* **150**, 711–721 (1998).

34. Wang, J. W., Wong, A. M., Flores, J., Vosshall, L. B. & Axel, R. Two-photon calcium imaging reveals an odor-evoked map of activity in the fly brain. *Cell* **112,** 271–282 (2003).
35. Lee, T. & Luo, L. Mosaic analysis with a repressible cell marker for studies of gene function in neuronal morphogenesis. *Neuron* **22,** 451–461 (1999).
36. Kiefer, C., Sumser, E., Wernet, M. F. & Von Lintig, J. A class B scavenger receptor mediates the cellular uptake of carotenoids in *Drosophila*. *Proc. Natl Acad. Sci. USA* **99,** 10581–10586 (2002).
37. Rong, Y. S. *et al.* Targeted mutagenesis by homologous recombination in *D. melanogaster*. *Genes Dev.* **16,** 1568–1581 (2002).
38. Jones, W. D., Cayirlioglu, P., Kadow, I. G. & Vosshall, L. B. Two chemosensory receptors together mediate carbon dioxide detection in *Drosophila*. *Nature* **445,** 86–90 (2007).
39. de Bruyne, M., Clyne, P. J. & Carlson, J. R. Odor coding in a model olfactory organ: the *Drosophila* maxillary palp. *J. Neurosci.* **19,** 4520–4532 (1999).